

OXYGEN ISOTOPE MICROANALYSIS BY SECONDARY ION MASS SPECTROMETRY SUGGESTS CONTINUOUS 300-MILLION-YEAR HISTORY OF CALCITE CEMENTATION AND DOLOMITIZATION IN THE DEVONIAN BAKKEN FORMATION

MARK W. BRODIE,¹ ANDREW C. APLIN,¹ BRUCE HART,² IAN J. ORLAND,³ JOHN W. VALLEY,³ AND ADRIAN J. BOYCE⁴

¹Department of Earth Sciences, Durham University, Durham DH1 3LE, U.K.

²Statoil Gulf Services LLC, 6300 Bridge Point Parkway, Austin, Texas 78730, U.S.A.

³WiscSIMS, Department of Geoscience, University of Wisconsin–Madison, Madison, Wisconsin 53706, U.S.A.

⁴Scottish Universities Environmental Research Centre, Rankine Avenue, East Kilbride G75 0QF, U.K.

e-mail: a.c.aplin@durham.ac.uk

ABSTRACT: Calcite cementation and dolomitization are key diagenetic processes in many sedimentary systems. Unravelling detailed histories and timescales of cementation and replacement is, however, often compromised by the limited spatial resolution of many analytical techniques; in some cases multiple grains are co-analyzed so that diagenetic histories are blurred and reaction periods are difficult to establish. In this study we have used 10-micrometer-resolution, *in situ* secondary ion mass spectrometry to determine the oxygen isotope composition of 197 individual, 10–50-micrometer-size crystals of dolomite and calcite from six samples in a single core of Upper Devonian middle Bakken Member siltstones and sandstones, the major tight oil formation of the Williston basin, USA. This amount of data places important constraints on the range of temperatures and times that carbonate cementation and replacement occurred. Petrographic data show that microcrystalline calcite cement is an early phase, and combined with mineralogical data suggest that much of the dolomite replaces calcite. Over spatial scales of less than a centimeter, analyses of individual calcite crystals have a range of 5‰ for $\delta^{18}\text{O}$ in the group of crystals, and for the group of individual dolomite crystals, 10‰. These sub-centimeter ranges are as great as those observed in previous studies of carbonate cements sampled over many meters and remind us that previous low-resolution studies may have inadvertently analyzed mixed phases. There is no relationship between dolomite texture and isotopic composition at this spatial scale; microscale backscattered electron imagery and scanning electron microscopy cathodoluminescence zoning is seen, but cannot be resolved with a 10-micrometer spot size. Assuming, since it is an early cement, that calcite precipitated from seawater ($\delta^{18}\text{O} = -1.5\text{‰}$), it formed at *ca.* 15–40°C, mainly at the lower temperatures. Present-day formation waters in Devonian rocks in this region have oxygen isotope compositions of 7–8‰ VSMOW. Using these values as a likely dolomitizing fluid, we suggest that dolomitization occurred continuously between 40 and 140°C over 150–200 million years, most likely in a fluid with a high Mg/Ca ratio resulting from gypsum formation in local evaporites. We suggest that this exceptionally low rate of dolomitization was controlled by the low rate of supply of Mg in a very sluggish flow regime; dolomitization is incomplete because of a limited supply of Mg.

INTRODUCTION

Burial diagenesis transforms sediments into sedimentary rocks through a range of mechanical and chemical processes driven by changes in effective stress and the requirement that mineral assemblages attempt to achieve thermodynamic equilibrium as a function of temperature, pressure, and fluid composition (e.g., Bjørlykke 2014). Although the chemical diagenetic reactions are wide-ranging, depending for example on initial mineralogy and fluid chemistry, questions which are generic to all processes involve (a) the rate of reactions, (b) the extent to which a pre-defined “system” (for example a sand body) is chemically open or closed, and (c) whether or not the reactions occurred continuously or were punctuated (e.g., Giles 1997; Burley et al. 1989; Giles et al. 2000; Gluyas and Coleman 1992; Robinson and Gluyas 1992; Taylor et al. 2010; Bjørlykke and Jahren 2012; Bjørlykke 2014).

These fundamental questions continue to be asked, in part at least, because of limitations in the analytical techniques available to answer them. Many studies have used some combination of petrography, fluid inclusions, and stable isotopes to evaluate diagenetic histories (e.g., Haszeldine et al. 1984; Land et al. 1987; Glasmann et al. 1989; Brint et al. 1991; Aplin and Warren 1994; Williams et al. 1997; Sullivan et al. 1997; Taylor et al. 2000; Girard et al. 2001; Goldstein 2001; Marchand et al. 2002; Schmid et al. 2004). However, diagenetic silicate and carbonate minerals in sandstones commonly form grains or overgrowths on scales less than 100 micrometers and may have grown over many millions of years. Detailing growth histories of individual phases thus requires probes which can operate on a sub-10-micrometer scale. Conventional stable-isotope and fluid-inclusion studies cannot unravel these histories because (a) the resolution of isotopic analyses is insufficient and (b) fluid inclusions tend to occur in specific locations of diagenetic phases, for example at

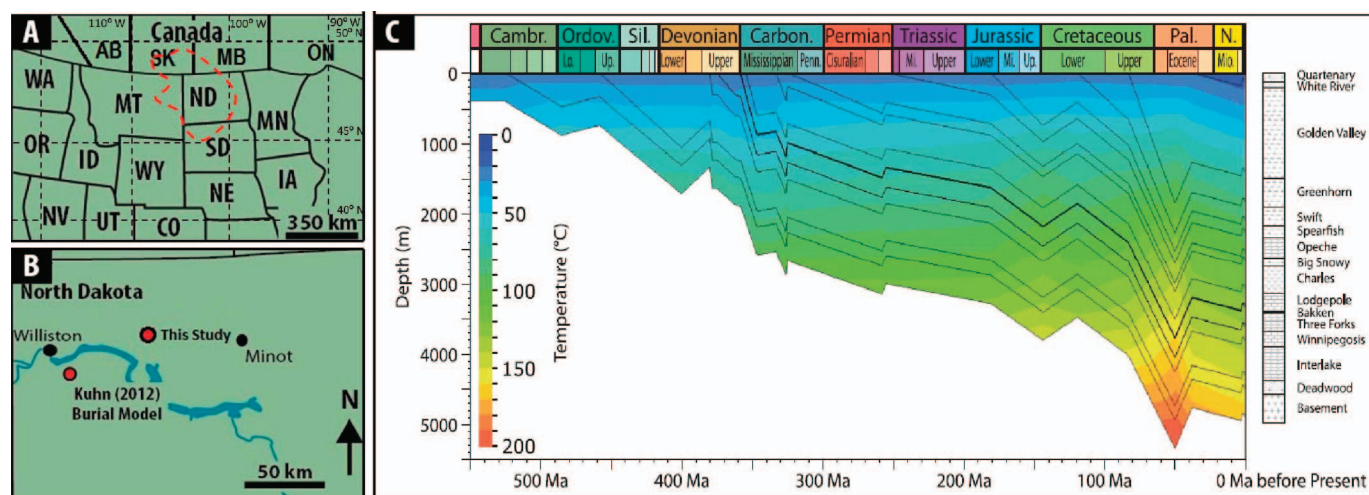


FIG. 1.—A) Map of northern USA and southern Canada showing states and provinces. ND, North Dakota. B) Map of North Dakota, showing the location of the well in this study and that modeled in the Kuhn et al. (2012) study. Williston Basin is outlined in red. C) Burial history of the Williston basin developed for the basin center in North Dakota. The temperature through time is overlaid. Camb., Cambrian; Ordov., Ordovician; Sil., Silurian; Carbon., Carboniferous; Pal., Paleogene; N., Neogene; Up., Upper; Mi., Middle; Lo., Lower; Penn., Pennsylvanian; Mio., Miocene. From Kuhn et al. (2012).

grain-overgrowth boundaries or in healed microfractures (e.g., Osborne and Haszeldine 1993).

Oxygen isotopes preserve important information about the temperature at which minerals form and the nature of the fluids from which they precipitate. Earlier isotopic studies on diagenetic quartz and carbonate were made on whole overgrowths or areas sampled with microdrills, and could not generate temporal data (Lee and Savin 1985; Land et al. 1987; Brint et al. 1991; Hart et al. 1992; Macaulay et al. 1993; Aplin and Warren 1994; Taylor et al. 2000; McBride and Milliken 2006). *In situ* isotope studies on well-identified minerals can overcome uncertainties of what is being analyzed, but neither the resolution (20–30 μm) nor the precision ($\pm 2\%$; 2SD) of earlier work using single-collector secondary ion mass spectrometers (SIMS) were sufficient to constrain growth histories (Graham et al. 1996; Williams et al. 1997; Lyon et al. 2000; Girard et al. 2001; Marchand et al. 2002). Technical advances in SIMS now allow *in situ* analyses to be made on 2–10- μm -diameter regions and have revealed up to 10‰ ranges in $\delta^{18}\text{O}$ in single quartz overgrowths and carbonate cements (Pollington et al. 2011; Harwood et al. 2013; Śliwiński et al. 2016b).

Carbonates are common and often pervasive cements in marine sandstones (e.g., Bjørkum and Walderhaug 1990, 1993; Macaulay et al. 1993; Klein et al. 1999; Taylor et al. 2000; McBride and Milliken 2006). Although significant carbonate cement can be formed during early burial (e.g., Bjørkum and Walderhaug 1990, 1993), oxygen and carbon isotope data often show a wide range of values which imply a range of precipitation temperatures and/or fluid compositions (e.g., Klein et al. 1999; Taylor et al. 2000). However, detailed petrography, for example using backscattered electron microscopy, commonly reveals chemically distinct carbonate phases on a sub-millimeter scale (e.g., Hart et al. 1992; Taylor et al. 2000; Śliwiński et al. 2016b). This means that conventional isotope analyses, in which areas of at least a few millimeters are sampled, are likely to result in the analysis of mixed phases or of a single phase that has grown over a long period of time. Equally, studies which have used selective leaching to isolate compositionally distinct carbonate phases rely on the specificity of the leaching method (e.g., Macaulay et al. 1993; Klein et al. 1999). The nature of these analytical tools means that diagenetic histories are inevitably blurred or uncertain.

Dolomite and calcite grains examined in this study of the Upper Devonian middle Bakken Member in North Dakota are often smaller than

100 micrometers. The use of high-resolution SIMS, an analytical tool which allows oxygen isotope data to be collected from areas 10 micrometers in diameter, is thus essential if the timing and evolution of fluids responsible for the formation of these diagenetic phases are to be unraveled accurately. The Bakken Formation has recently received much attention as a highly significant unconventional hydrocarbon accumulation, and the occurrence of both calcite and dolomite is central to the quality of the petroleum reservoir (e.g., Li et al. 2015). Previous work on the oxygen-isotope composition of carbonates in the Bakken has been limited to studies of calcite in fracture fills (Pitman et al. 2001), the bulk analysis of mixed carbonates (Karasinski 2006), and one grain-scale study (Staruijala et al. 2013). Here, we report oxygen isotope data obtained by SIMS on calcite and dolomite grains and focus on four questions: (a) over what temperature and period of time did the carbonate phases form; (b) was carbonate diagenesis continuous or punctuated; (c) is the dolomite a primary cement or did it form through dolomitization of earlier calcite (e.g., Warren 2000; Machel 2004); and (d) to what extent did diagenesis occur in a closed or open geochemical system?

GEOLOGICAL CONTEXT

The Upper Devonian–Lower Mississippian Bakken Formation was deposited over wide areas of the intracratonic Williston basin, which covers 770,000 km^2 of Montana, North Dakota, and South Dakota in the USA and parts of Saskatchewan and Manitoba in Canada (Fig. 1). The basin is structurally simple with an almost complete stratigraphic section and only gentle, low-wavelength folding (Webster 1984; Meissner 1991). The burial history, based on a well which has a stratigraphy very similar to that of the core used in this study and in which the Bakken is buried to essentially the same depth, is one of continual subsidence from deposition to ca. 50 Ma, followed by modest uplift and renewed subsidence from 35 Ma to the present day (Kuhn et al. 2012) (Fig. 1C). The present-day temperature for the samples of this study is around 125°C with a modeled maximum temperature between 150 and 160°C.

The Bakken is divided into three stratigraphic members (Fig. 2). The Upper and Lower members are both organic-rich shales whilst the middle Bakken Member, the subject of this study, comprises a variably but often highly carbonate-cemented series of very fine-grained sandstones and siltstones deposited over large areas of a shallow, epicontinental sea

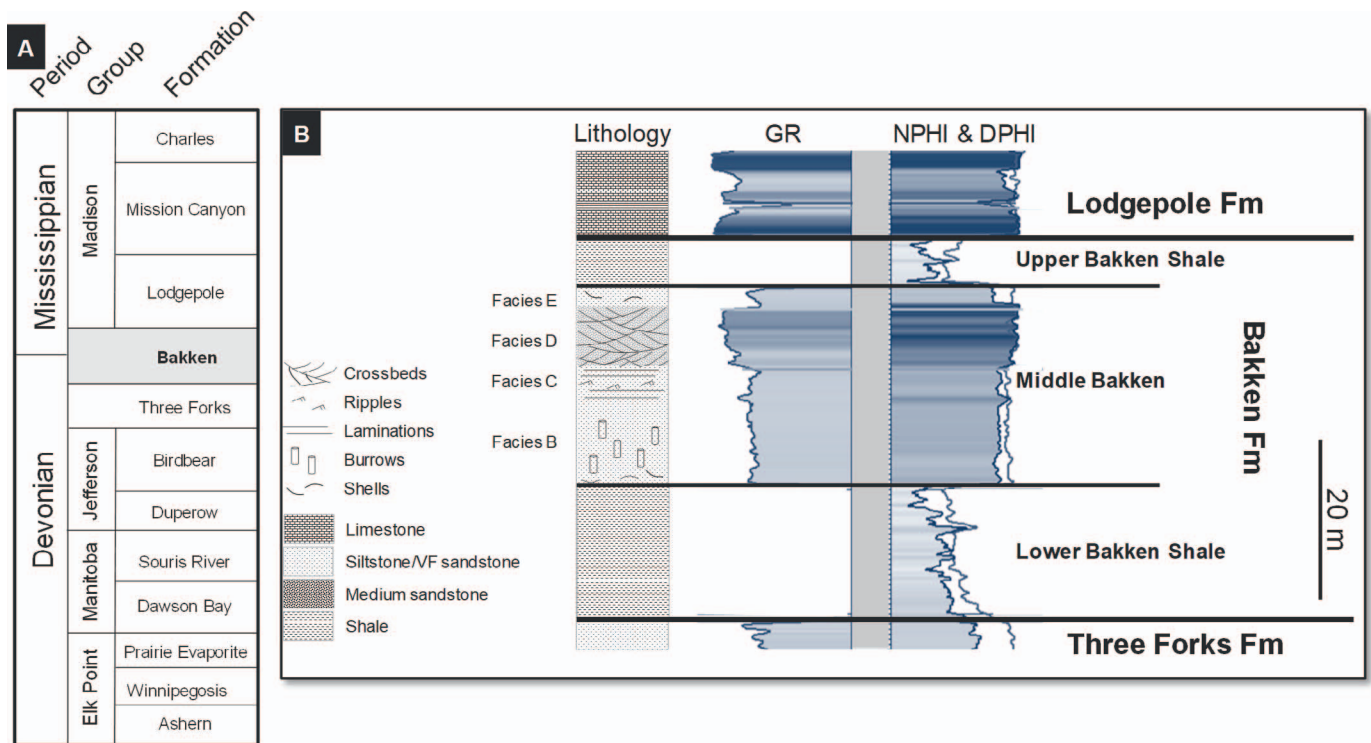


FIG. 2.—**A**) Stratigraphic column of the Devonian–Mississippian strata overlying and underlying the Bakken Formation. **B**) Generalized lithological log showing the principal sedimentary structures in each facies, adjacent to which are the gamma-ray (GR), neutron-porosity (NPHI), and density-porosity (DPHI) logs.

(Meissner 1978; Freisatz 1995; Egenhoff et al. 2011). At the depocenter of the Williston basin the middle Bakken reaches a maximum thickness of 46 m but varies in thickness across the basin (Pitman et al. 2001). Most current work suggests that the middle Bakken was deposited in a variety of shallow-marine environments during a Late Devonian to Early Mississippian regression (e.g., Li et al. 2015). Whilst the sedimentology of the middle Bakken has been extensively described (McCabe 1959; Meissner 1978; Webster 1984; Holland et al. 1987; Smith and Bustin 1996; Pitman et al. 2001; Egenhoff et al. 2011; Egenhoff 2017), diagenetic studies are more limited. Nevertheless, pervasive early calcite cement has been recognized in several studies (Last and Edwards 1991; Pitman et al. 2001; Ferdous 2001; Li et al. 2015), along with the interpretation of several phases of dolomite (Ferdous 2001).

EXPERIMENTAL METHODS

Samples

Samples for this study come from a single core drilled in McKenzie County, North Dakota, USA (Fig. 1B). The core was described using the five facies associations defined by Simenson (2010) in a study of the middle Bakken from the Parshall Field, Mountrail County, North Dakota. A total of 32 core plugs were taken over the full thickness of the middle Bakken section; six of the 32 samples were selected for this study, including samples from each of the five different facies.

Petrography

Thin sections were cut perpendicular to bedding from core plugs and carbonate textures investigated using both transmitted-light and electron microscopy. Transmitted-light microscopy was carried out using a Nikon Eclipse 50iPOL polarizing microscope. 300 points per sample were counted using a Petroglight petrographic point counter. The thin sections

were then coated with a 30 nm layer of carbon before analysis by electron microscopy. Electron microscopy was performed at Durham University's GJ Russell Electron Microscopy Facility on a Hitachi SU 70 FEG SEM in secondary (SE) and backscatter (BSE) and Cathodoluminescence (CL) modes. Images were acquired at 15 kV, 2–4 nA, and a working distance of 15–16 mm.

Dolomite crystal textures were classified using the scheme described by Sibley and Gregg (1987). Whilst proposed principally for dolomite crystals in carbonate rocks, this scheme is also appropriate for low-temperature, mixed clastic–carbonate systems like the Bakken because it focuses on the grain-boundary and grain-size relationships of individual crystals, which can be used to infer the genetic origin of each dolomite crystal class.

Scanning Electron Microscopy–Cathodoluminescence (SEM-CL) images were acquired on carbon-coated thin sections and round resin plugs using the Hitachi SU 70 FEG SEM with a Gatan Mono-CL detector operated in panchromatic mode. Images were obtained at an accelerating voltage of 10 kV and a working distance of 17 mm. Spectral information was obtained over a wavelength search range of 505–800 nm and a dwell time of approximately 3,200 μ s per pixel for an image resolution of 2250 \times 2250. Intensity values were corrected using the system response curve.

Using SEM-WDS, the elemental compositions of 58 calcite crystals and 155 dolomite crystals with different textures in 13 samples were determined, including the six samples on which SIMS analyses were performed. Analyses were repeated three times per crystal, and the results for each crystal are reported as the mean of the three analyses.

Mineralogy

Bulk mineralogy was determined by KT Geoservices (Table 1). X-ray diffraction (XRD) analysis was conducted using a Siemens D500 automated powder diffractometer equipped with a copper X-ray source (40 kV, 30 mA) and a scintillation X-ray detector. Both bulk and clay (< 4

TABLE 1.—Mineralogical and bulk stable carbon and oxygen isotope data for calcite and dolomite obtained by sequential acid dissolution.

Oxygen and Carbon Isotopes by Sequential Acid Extraction									
Depth (m)	Sample No.	SIMS Sample No.	Facies	Calcite at 25°C			Dolomite at 100°C		
				Carbon ($\delta^{13}\text{C}_{\text{VPDB}}$) ‰	Oxygen ($\delta^{18}\text{O}_{\text{VSMOW}}$) ‰	Oxygen ($\delta^{18}\text{O}_{\text{PDB}}$) ‰	Carbon ($\delta^{13}\text{C}_{\text{VPDB}}$) ‰	Oxygen ($\delta^{18}\text{O}_{\text{VSMOW}}$) ‰	Oxygen ($\delta^{18}\text{O}_{\text{PDB}}$) ‰
969.93	1-36B	7	E	-0.2	26.4	-4.3	-0.5	25.7	-5.0
970.02	1-37B	N/A	E	-0.8	26.1	-4.6	-0.2	26.7	-4.0
970.10	1-38B	N/A	E	-2.5	23.7	-7.0	0.8	28.6	-2.2
970.21	1-39B	N/A	E	-0.4	26.5	-4.2	0.0	27.4	-3.4
970.98	2_iiA	6	D2	3.1	25.8	-4.9	1.5	28.7	-2.1
971.00	4_iiA	5	D2	3.8	27.1	-3.7	2.7	30.9	0.0
972.43	9_iiA	4	D1	3.3	26.0	-4.7	3.6	30.8	-0.1
973.95	17_iiA	3	C	2.0	24.4	-6.3	-0.3	26.1	-4.6
975.96	11_iiA	2	Grad	-0.5	25.3	-5.4	-0.5	27.0	-3.8
977.12	1-113B	N/A	B	-3.2	25.4	-5.3	-3.3	26.5	-4.2
977.17	1-114B	N/A	B	2.5	24.7	-6.0	-2.1	19.8	-10.7
977.27	1-115B	N/A	B	1.6	25.3	-5.4	-0.3	26.1	-4.6
977.36	1-116B	N/A	B	1.5	25.5	-5.2	-0.3	27.1	-3.7

Carbonate minerals calcite and dolomite were separated using conventional phosphoric acid digestion and gas-source mass spectrometric analyses on selected Middle Bakken samples. Calcite is considered to be the CO_2 extracted after three hours of acid digestion at 25°C in a vacuum, and dolomite is considered to be the CO_2 extracted after 24 hours at 100°C in a vacuum. Note that SIMS data from this study indicate that calcite and dolomite were not separated by this procedure. SIMS sample numbers are also shown.

μm) analyses were conducted. Quantitative data were obtained from the whole-rock pattern using whole pattern fitting (WPF) and Rietveld refinement methods.

Bulk C and O Isotope Analysis

The carbon and oxygen stable-isotope composition of bulk calcite and dolomite were analyzed at the Scottish Universities Environmental Research Centre (SUERC) on an Analytical Precision AP2003 mass spectrometer equipped with a separate acid injector system (Table 1). We attempted to separate calcite and dolomite through the preferential dissolution of calcite by reaction with 105% H_3PO_4 under a helium atmosphere at 70°C. As shown later, our results in fact indicate that the fine-grained dolomite in these samples was also substantially dissolved with this method. Measured O isotope ratios are reported as per mil deviations relative to Vienna standard mean ocean water (VSMOW) and C isotopes relative to Vienna PeeDee Belemnite (VPDB) using conventional delta (δ) notation. Mean analytical reproducibility based on replicates of the SUERC laboratory standard MAB-2 (Carrara Marble) was around $\pm 0.2\text{‰}$ for both carbon and oxygen. MAB-2 is an internal SUERC laboratory standard extracted from the same Carrara Marble quarry as the IAEA-CO-1 international standard. It is calibrated against IAEA-CO-1 and NBS-19 and has exactly the same C and O isotope values as IAEA-CO-1 (-2.5‰ and 2.4‰ VPDB, respectively).

Secondary Ion Mass Spectrometry

In-situ, sub-grain-scale oxygen stable-isotope data were obtained using secondary ion mass spectrometry. Based on their mineralogy and petrographic characteristics, six representative samples were selected, one from each facies. Soluble organic matter was removed using a standard, 96 hour soxhlet extraction procedure using a mixture of dichloromethane and methanol. The samples were then mounted in epoxy resin in 1-inch round plugs. Several crystals (2 or 3) of calcite standard UWC-3 ($\delta^{18}\text{O}_{\text{VSMOW}}$ of UWC-3 is $12.49\text{‰} \pm 0.03\text{‰}$ 1 SD, $n = 9$; Kozdon et al. 2009) were mounted at the center of each sample. The sample was then polished sequentially with 6 μm , 3 μm , and 1 μm diamond paste on a low-nap pad.

The final polish was obtained using a 0.05 μm colloidal alumina solution on a vibrating pad for 30–200 seconds. The polished sample plugs were then gently cleaned with deionized water and ethanol, and dried in a vacuum oven for 5 hours at 40°C. To prevent charging during analysis, samples were coated with 60 nm gold. The flatness across the samples was measured using a white-light profilometer across both the polished rock, the mounted and polished calcite standard, and enclosing epoxy. The maximum topography recorded was 3 μm (sample) and 7 μm (sample and standard). Analysis spots were not placed near localized areas with relief $> 3 \mu\text{m}$.

In-situ oxygen isotope data were acquired using a CAMECA IMS 1280 large-radius multi-collector ion microprobe at the WiscSIMS Laboratory at the University of Wisconsin–Madison (Kita et al. 2009; Valley and Kita 2009). A $^{133}\text{Cs}^+$ primary ion beam with a current of 1.4 nA was focused at the analytical surface, resulting in ellipsoidal pits ca. 10 $\mu\text{m} \times 13 \mu\text{m}$ in size. The typical secondary $^{16}\text{O}^-$ ion intensity for the 300 analyses of this study was approximately 2.5×10^9 cps.

Both before and after every set of 8–17 sample analyses, a sample-mounted calcite standard (UWC-3) was measured four times. As for conventional analyses, stable-isotope ratios are reported using the standard delta notation relative to VSMOW ($\delta^{18}\text{O}\text{‰}$). The reproducibility of each set of unknown samples is reported as 2 SD of the bracketing standard analyses; the average 2 SD of bracketed analyses was 0.27‰ (refer also to the Supplemental Material). Detailed analytical protocols can be found in Kita et al. (2009).

Initial SEM-EDX observations indicated the presence of iron in some of the dolomite crystals. Śliwiński et al. (2016a) show that the extent of isotopic fractionation occurring during SIMS analysis of carbonates (matrix effect) is a function of the concentration of iron. Thus, instrument standards for the dolomite–ankerite series were analyzed during the same SIMS session to ensure the accuracy and precision of analyses for the full range of potential carbonate chemistries. In addition, the carbonate in each pit analyzed by SIMS was identified in the SEM, and the iron composition of the crystal measured using SEM-WDS (adjacent to the pit), using an INCA Wave 700 spectrometer WDS detector attached to a Hitachi SU-70 FEG SEM. The SEM “spot size” (beam diameter) was between 1.7 and 5 nm with an interaction depth of up to 800 nm and width of around 3 μm .

TABLE 1.—Extended.

Depth (m)	XRD Mineralogy (wt %)								
	Quartz	Illite & Mica	Potassium Fspar	Plagioclase Fspar	Calcite	Dolomite	Pyrite	Halite	Chlorite
969.93	42	13	4	5	3	29	2	2	0
970.02	33	16	4	5	3	37	2	1	0
970.10	19	4	2	2	56	16	1	0	0
970.21	28	10	4	3	7	47	1	0	0
970.98	46	3	4	2	31	14	1	0	0
971.00	46	4	3	1	30	15	1	0	0
972.43	38	5	6	3	36	12	0	0	0
973.95	45	8	8	5	14	21	1	0	0
975.96	31	6	5	4	11	42	1	0	0
977.12	18	11	4	3	21	41	1	1	1
977.17	29	12	4	3	37	12	2	0	1
977.27	23	10	3	3	53	5	3	0	1
977.36	30	13	4	3	36	9	3	0	1

To ensure that the analyses were of specific crystals, only crystals with the shortest visible length of $> 2 \mu\text{m}$ were analyzed. Three sets of standards were used for SEM-WDS: (a) an elemental cobalt instrument standard was used at the start of every session; (b) at the start and end of each analytical session, the calcite standard UWC-3 (see Kozdon et al. 2009) which was mounted to the center of all of the analyzed samples was measured five times; (c) a series of carbonate standards with known chemical compositions (calcite, ankerite, dolomite, and siderite) were analyzed to measure accuracy and precision (see Supplemental Material). Using the results of SEM-WDS analysis, we used the mass bias calibration method proposed by Śliwiński et al. (2016a) to correct SIMS $\delta^{18}\text{O}$ measurements for the presence of iron in the dolomite crystals (Supplemental Material). Only 8 analyses required correction for the presence of iron, since iron contents were generally less than the detection limit of 0.1 wt. % FeO. The residual of the dolomite–ankerite calibration curve, fitted through seven standard materials measured during the same SIMS session, was 0.25%.

RESULTS

Sedimentology, Mineralogy, and Petrography

The middle Bakken is a sedimentologically heterogeneous fine sandstone–siltstone unit that is pervasively but variably cemented by both calcite and dolomite. Using the framework provided by Simonsen (2010) and the sedimentologic description of this core by Li et al. (2015), five facies (B, C, D1, D2, and E) were defined from the base (3206 m) to the top (3182 m) of the core, with a gradational facies between B and C. Facies B comprises strongly bioturbated, argillaceous, calcareous sandstones and siltstones; facies C consists of very fine-grained sandstones and siltstones showing both planar and undulose lamination, with some thin mud-rich horizons; facies D1 is a fine-grained sandstone with common soft-sediment deformation features; facies D2 consists of a light brown to light gray, parallel to undulating-laminated, low-angle cross-laminated sandstone; facies E comprises a dark gray siltstone interbedded with a light gray, thinly parallel-laminated, very fine-grained sandstone.

Core photographs taken with both white and UV light (Fig. 3) suggest that in all facies, there are multiple 2–30-cm-thick zones of layered or nodular diagenetic carbonate where porosity has been infilled to the extent that they do not contain fluorescing oil (i.e., calcite cementation pre-dated oil migration; Li et al. 2015). Other areas, which do contain fluorescing oil, are more lightly and/or more variably carbonate-cemented. Based both on

the XRD analysis of 13 samples and point counting of 15 samples, calcite (both primary, bioclastic calcite, and diagenetic calcite) constitutes 3–56% of the rock volume and diagenetic dolomite between 5 and 41% (Table 1). Total carbonate content (calcite plus dolomite, including bioclastic calcite) varies between 32 and 72%. The average minus-cement porosity is 42% (range 36–46%), close to depositional porosity, and suggesting that cementation started close to the sediment–water interface. The inverse correlation between the amounts of calcite and dolomite ($r^2 = 0.62$) lends support to the idea that dolomite is replacing calcite rather than being a primary cement.

At the core scale, calcite- and dolomite-cemented regions are present in approximately 70% of the core. In thin section, diagenetic calcite and dolomite cement occurs as bands. These bands vary in thickness from a couple of millimeters up to the size of the full section. Whilst in most instances the millimeter-scale bands form sharp contacts parallel to bedding, in some cases there is no clear lithological control on the morphology of the contact or the spatial distribution within the section.

Diagenetic calcite is observed in two textural types. By far the most volumetrically important texture (Type 1) is pervasive, poikilotopic cement in which detrital grains “float” within the calcite (Figs. 4D, 5A). Similar, early, massive calcite cement is common in shallow-marine sandstones (e.g., Bjørkum and Walderhaug 1993). Type 2 calcite comprises individual crystals which (a) appear to cement small numbers of grains to form a globular morphology (Fig. 5B), and (b) occur as individual, discrete grains which do not connect other grains; visual estimates from SEM show that these phases form $< 1\%$ of calcite.

Dolomite occurs as six different morphologies. Type 1 dolomites are nonplanar, anhedral crystals with rounded edges, 15–30 μm in size (Fig. 6A). Type 2 dolomites are euhedral rhombs, 10–50 μm in size with micrometer-scale pores in their core (Fig. 6B). Type 3 dolomites are euhedral rhombs, 10–50 μm in size but without pores (Fig. 6C). Type 4 dolomites are subhedral, geometric, angular crystals which vary in size from 5 to 35 μm (Fig. 6D). Type 5 dolomites are 2–10- μm -thick ferroan rims which form around more stoichiometric, iron-poor dolomite. This phase has been observed around all other dolomite types (Fig. 6E). Type 6 dolomites are euhedral rhombs which are less than 5 μm in diameter (Fig. 6F). Under transmitted light, some dolomites show a “cloudy core” texture which has been previously suggested to result from the dolomitization of a calcite precursor, resulting in a close-to-stoichiometric dolomitic outer

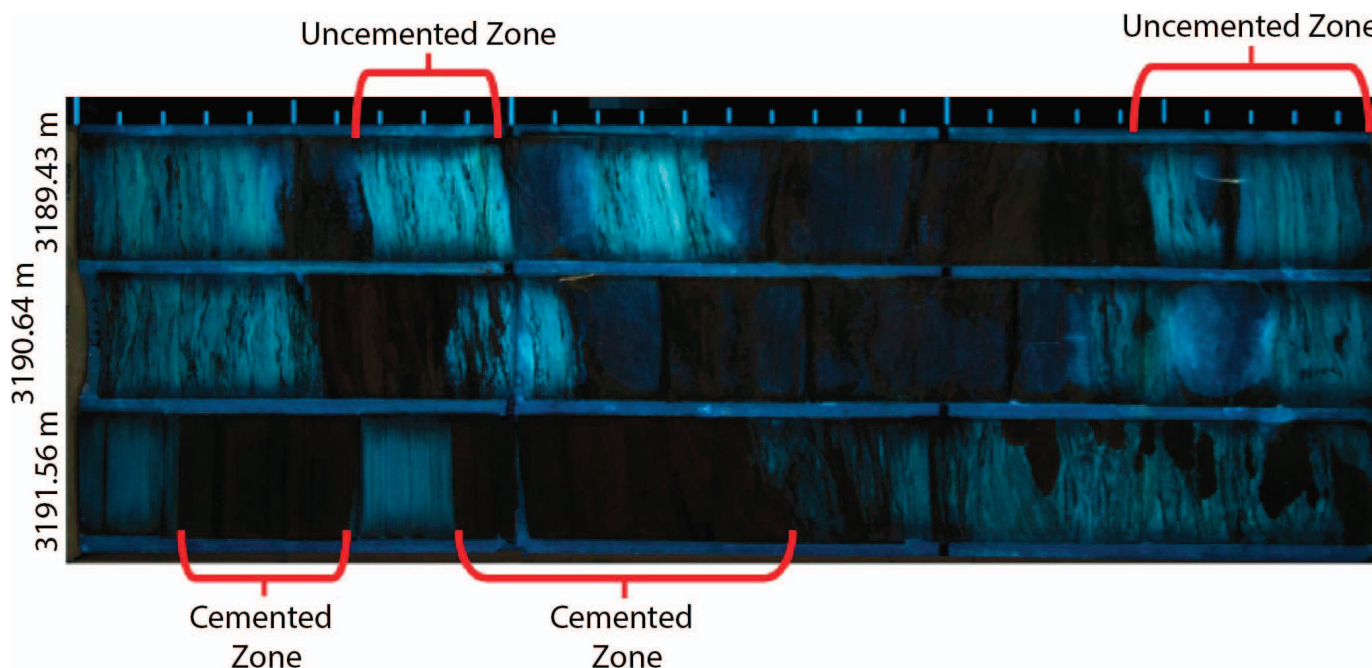


Fig. 3.—Core photograph taken with UV light of a section of the middle Bakken (facies D1). Fluorescing zones indicate oil-bearing sandstones and siltstones. Calcite-cemented sandstones correspond to segments of the core showing no or low fluorescence. Ticks on ruler represent 10 cm.

zone and a more calcium-rich and porous core (Murray and Lucia 1967; Sibley 1982).

In most cases, except in the relatively unusual cases of Fe enrichment towards the edge of crystals, BSEM shows no evidence of significant changes in the chemical composition of dolomite crystals from core to edge. Scanning electron microscopy–cathodoluminescence (SEM-CL) does however reveal zoning within individual dolomite crystals. Zones of different luminescence can reflect both subtle changes in crystal chemistry and/or variations in growth mechanisms (e.g., Boggs and Krinsley 2006), and our data are insufficient to determine the reasons for the zonation. In total, 48 crystals were viewed in 10 samples. The CL character of individual dolomite types was consistent in all the samples and is reported in Figure 7. All dolomite phases luminesce in the red part of the spectrum, including the “dull” zones which simply have a lower-intensity luminescence (Fig. 7). Anhedral, Type 1 dolomites show incomplete concentric zones which have decreasing luminescence intensity towards the edge of the crystals. Textural types 2–4 and 6 exhibit similar CL characteristics: a single, concentric, low-intensity luminescence zone around a much more intensely luminescing core. The rims are approximately 1–10 μm in thickness (Fig. 6E). Type 5 dolomites are ferroan rims which form single homogeneous layers around other dolomite crystals; they show low emission intensity in the red spectrum.

Chemical Composition

Calcite cement has a very consistent chemistry, averaging 97.4 mol % Ca, 2.4 mol % Mg, and 0.2 mol % Fe (Fig. 8). Eighty percent of dolomite analyses have chemical compositions between $\text{Ca}_{0.55}\text{Mg}_{0.45}\text{CO}_3$ and $\text{Ca}_{0.45}\text{Mg}_{0.55}\text{CO}_3$, with a modal value close to that of stoichiometric dolomite. There is no obvious relation between dolomite composition and textural type (Fig. 8). Almost all dolomites have low iron contents, with 85% containing less than 2 mol % Fe and only 2% with more than 6 mol % Fe. Note however that because of their spatial scale, Type 5 dolomites (ferroan dolomite rims) were not systematically measured, although they

quite commonly form either as discrete rims or more diffuse alteration zones around all other textural types of dolomite; they also form small, individual crystals with anhedral to euhedral habits.

Diagenetic dolomite containing more than 55 mol % Mg are uncommon in the literature; however, in this study, 17% of the analyses are more Mg-rich than $\text{Ca}_{0.45}\text{Mg}_{0.55}\text{CO}_3$. Most of these analyses are from samples 2 and 4, and the most common chemistry is around $\text{Ca}_{0.4}\text{Mg}_{0.6}\text{CO}_3$, i.e., between the composition of stoichiometric dolomite ($\text{Ca}_{0.5}\text{Mg}_{0.5}\text{CO}_3$) and huntite ($\text{Ca}_{0.25}\text{Mg}_{0.75}\text{CO}_3$).

Bulk C and O Isotope Composition

The results of bulk carbon and oxygen isotope analyses are reported in Table 1. The ranges for putative calcite and dolomite overlap substantially and are approximately -3 to $+3\text{‰}$ for carbon and $+20$ to $+30\text{‰}$ for oxygen (putative dolomite) and $+22$ to $+26\text{‰}$ (putative calcite). We use “putative” because with the benefit of the SIMS oxygen isotope analyses of individual calcite and dolomite crystals (see below) it is clear that the selective leach partially dissolved dolomite as well as calcite. This is readily understood, as, in practice, the “calcite” fraction is that gas extracted from the bulk samples after three hours of acid digestion in a vacuum; the “dolomite” fraction is the gas then extracted after a further 24-hour acid digestion on the residue (both corrected back to original carbonate as true calcite or dolomite). Whilst such “dolomite” analyses are likely to be free of calcite, the “calcite” is susceptible to contamination, as is shown by this study. Retrospectively, the advice is to proceed with caution when interpreting previous studies, which have used similar selective leaching techniques in an attempt to separate finely intergrown calcite and dolomite, particularly with the “calcite” data.

The main result of the bulk isotope analyses is that most of the carbon in both dolomite and (probably) calcite is from marine carbonate, with only minor inputs from organic sources. Values between -3‰ and $+3\text{‰}$ suggest the addition of relatively small amounts of organic carbon from processes involving coupled methanogenesis and CO_2 reduction, which would result

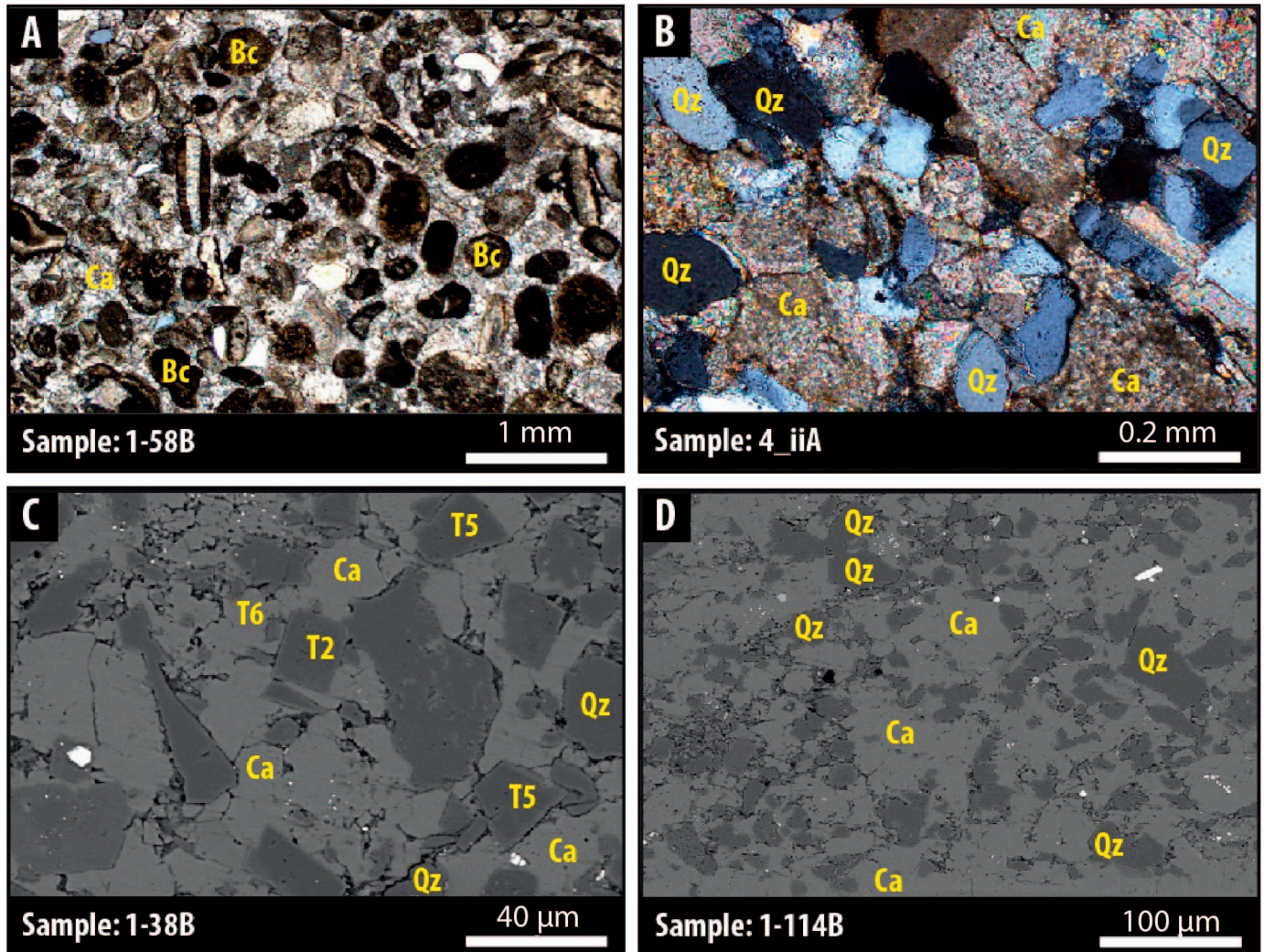


FIG. 4.—**A**) Bioclasts (Bc) in calcite (Ca) cement, showing a range of taxa including brachiopods, crinoids, and algal mats, viewed in XPL. **B**) Detrital quartz (Qz) grains floating in a calcite (Ca)-cemented zone, viewed under optical microscope in XPL. **C**) Small-scale, local cementation by calcite (Ca) cement and replacement dolomites of several morphologies (Type 2, T2; Type 5, T5; Type 6, T6) with an occasional detrital quartz (Qz) grain (BSEM). **D**) Larger-scale view of cementation of detrital quartz (Qz) grains by calcite (Ca) cement, viewed by SEM in BSE mode.

in more positive values, and from the oxidation of organic matter, which would result in more negative values (e.g., Curtis et al. 1986).

SIMS: Grain-Scale Oxygen Isotope Data

Three hundred and eight sites were analyzed from the six samples selected for SIMS analysis. After analysis, SEM was used to examine the shape of the pits formed by the ion beam. Previous work (Cavosie et al. 2005; Linzmeier et al. 2016) has shown that data from morphologically irregular pits are less reliable than those from regularly shaped pits. In this study we took a very strict approach to ensure that only the most reliable data were included. Some data were rejected due to the very fine nature of these samples, such that some mixed phases were measured. Most of the rejected data are in fact from crystals with minor irregularities such as surface asperities. All rejected data are reported in the Supplemental Material. Using these strict criteria, we accepted 197 analyses, i.e., between 16 and 46 analyses from six sample areas, each of which is approximately 5 mm in diameter.

Values of $\delta^{18}\text{O}$ for individual calcite grains are almost all between +28.9 and +33.7‰ (−1.9 to 2.8 ‰ VPDB), with a similar range in samples from

each facies (Fig. 9). For dolomite, the full range is +22.5 to 32.2‰ (−8.1 to 1.3 ‰ VPDB), with a mean value of +26.8‰ and with 93% of values between +24 and +30‰ (Fig. 9). There is a similar range of $\delta^{18}\text{O}$ values in each morphological type of dolomite. There is no relation between $\delta^{18}\text{O}$ and the Ca/Mg ratio of dolomite.

DISCUSSION

The oxygen isotope data in this study show as great a range on a sub-centimeter scale as many studies have found on conventional studies of diagenetic carbonates in sandstones sampled on scales of many meters (e.g., Bjørkum and Walderhaug 1993; Klein et al. 1999; Taylor et al. 2000). Given the sub-millimeter complexity observed in this study (Fig. 10), it is clear that conventional sampling methods can easily homogenize complex mixtures and result in an enforced, simplistic picture of diagenetic histories. Equally, however, our results show an overall commonality from sample to sample which show that carbonate diagenesis, although complex on a sample scale, proceeded in a similar way throughout fifteen meters of the middle Bakken. With SIMS, the large number of analyses of accurately identified mineral phases allows us to draw a temporal picture of

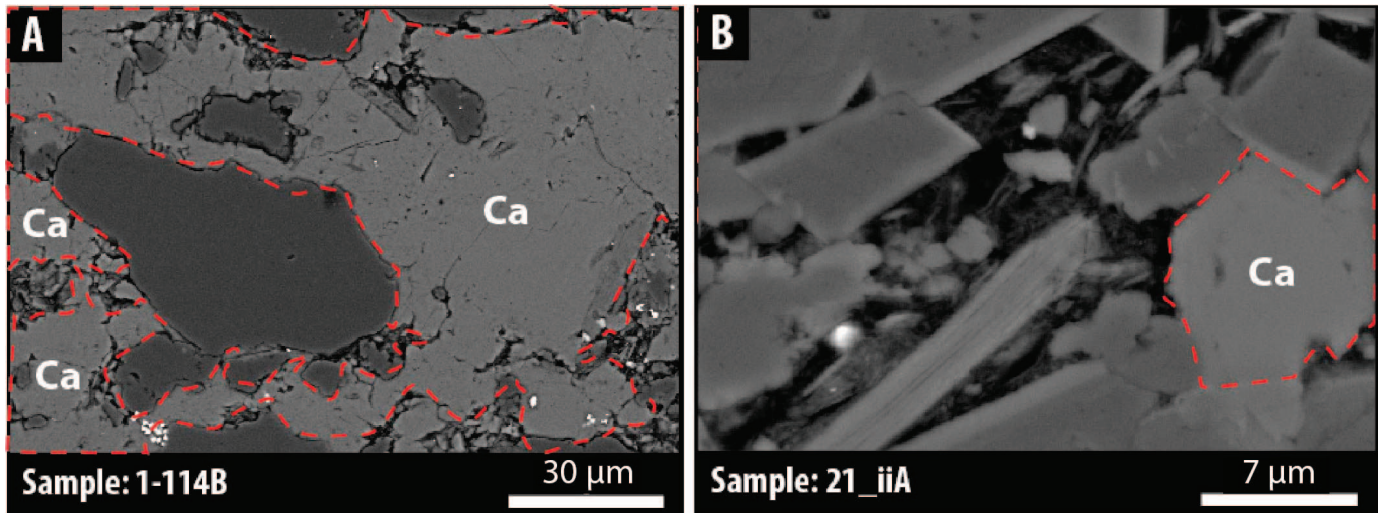


FIG. 5.—Backscattered electron micrographs of the various textural types of diagenetic calcite identified in the middle Bakken Formation. **A)** Type 1 calcite; forming a pervasive cement; **B)** Type 2 calcite; forming discrete grains, partially cementing other grains.

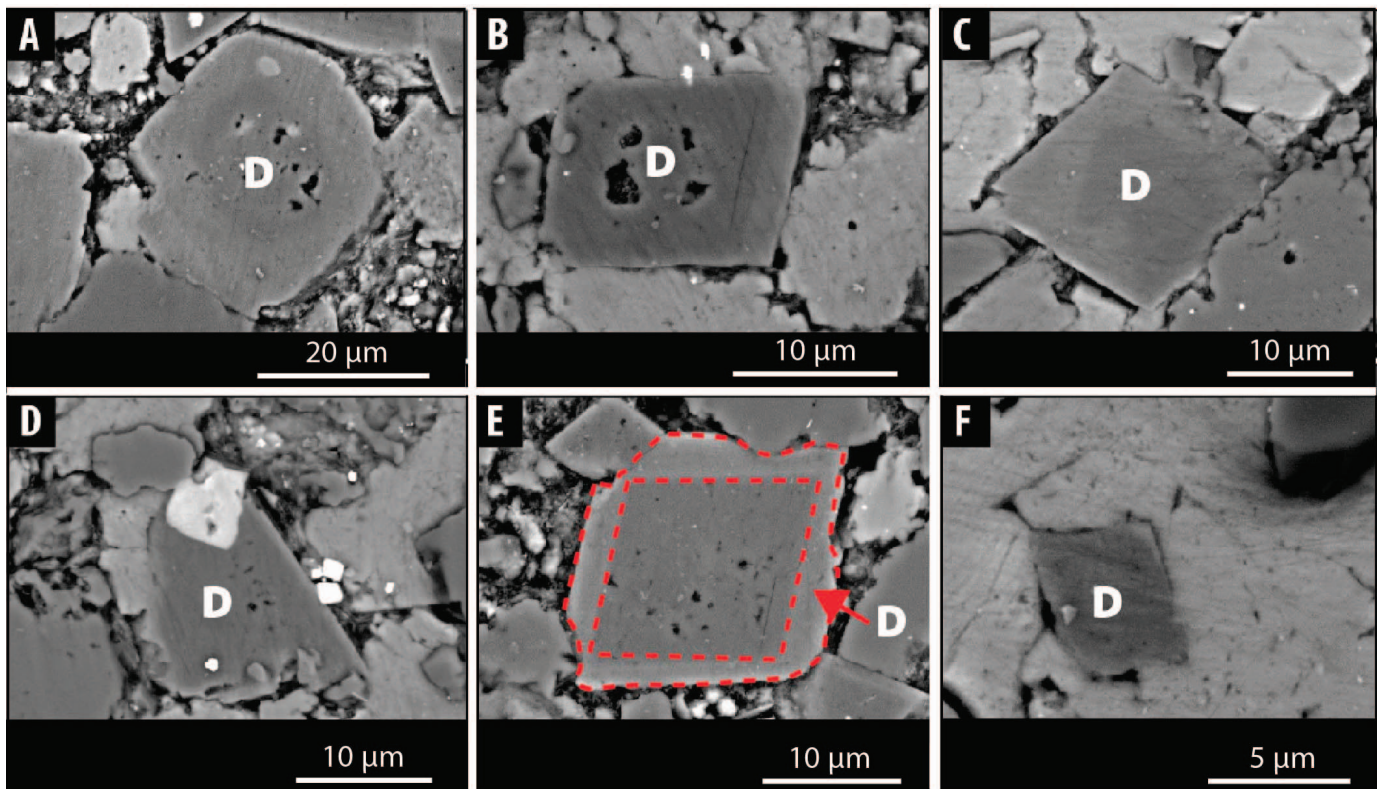


FIG. 6.—Backscattered electron micrographs of the various textural types of dolomite identified in the middle Bakken Formation. **A)** Type 1, non-planar dolomite; **B)** Type 2, planar-e with vuggy porosity; **C)** Type 3, planar-e; **D)** Type 4, planar-s; **E)** Type 5, ferroan-dolomite rims around dolomite; **F)** Type 6, planar-e (fine). In each case, D is the dolomite crystal of interest. Planar-e are euhedral dolomite, and planar-s are subhedral dolomite crystals (Sibley and Gregg 1987).

diagenesis which is not possible with conventional data. As we discuss below, our data suggest that carbonate diagenesis in the middle Bakken was not episodic but occurred continuously over an approximately 300-million-year period of burial.

High minus-cement porosities suggest that diagenetic calcite started to precipitate close to the sediment–water interface, as observed in many similar studies (e.g., Wilkinson 1991; Gluyas and Coleman 1992; Bjørkum

and Walderhaug 1990; 1993; Taylor et al. 2000). Our isotopic data support the early formation of calcite. Using the isotope paleothermometer proposed by O’Neil et al. (1969) for calcite and assuming a $\delta^{18}\text{O}$ of -1.5‰ for Late Devonian seawater (Hudson and Anderson 1989; van Geldern et al. 2006), the vast bulk of calcite formed between 15 and 35°C (Fig. 11).

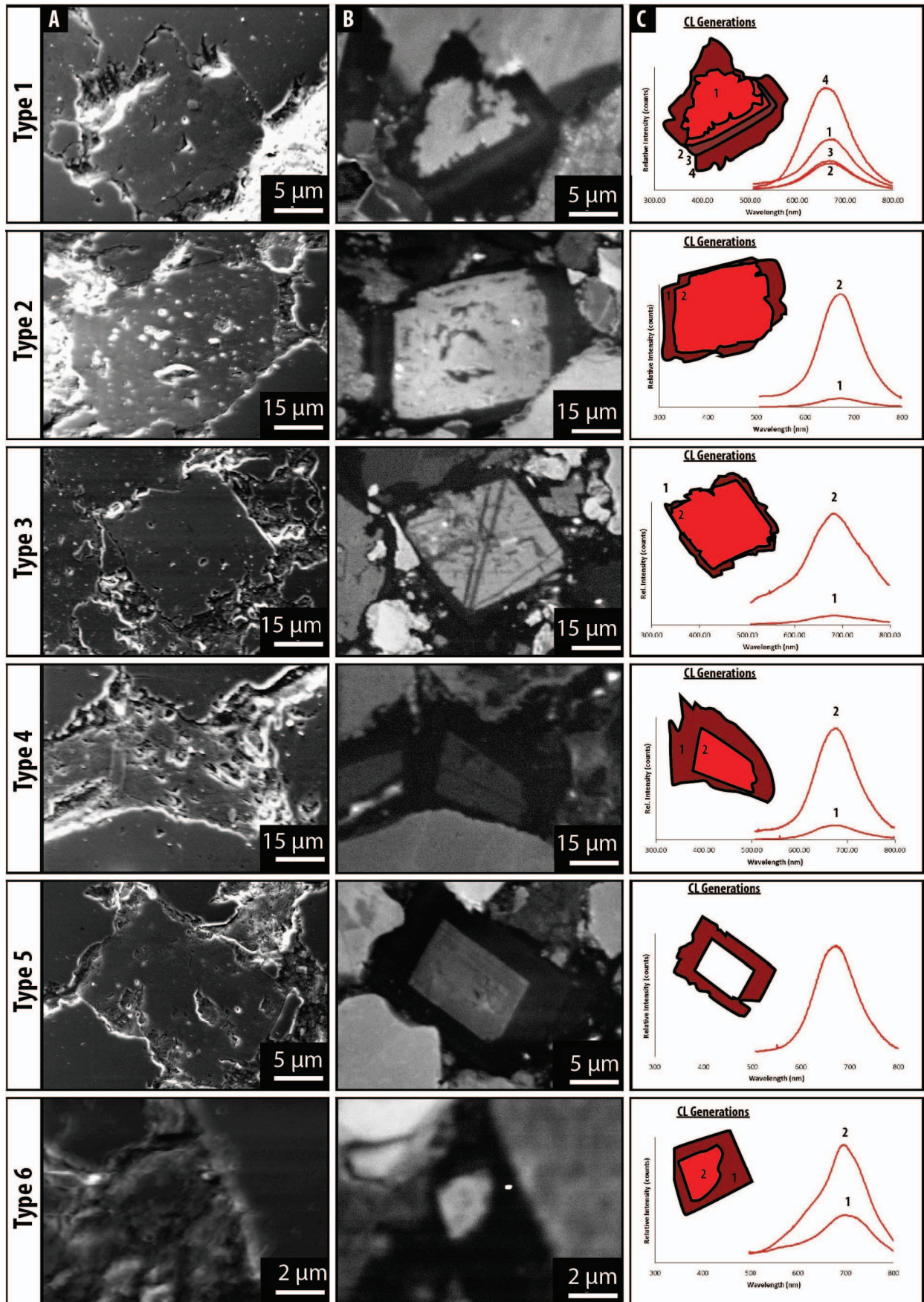


Fig. 7.—SEM-CL spectra of the six different dolomite textures: **A)** mixed SE-inline BSE image; **B)** SEM-CL image; **C)** Averaged CL spectra (for each zone) with schematic sketch of the CL generations and their relative luminescence (inset).

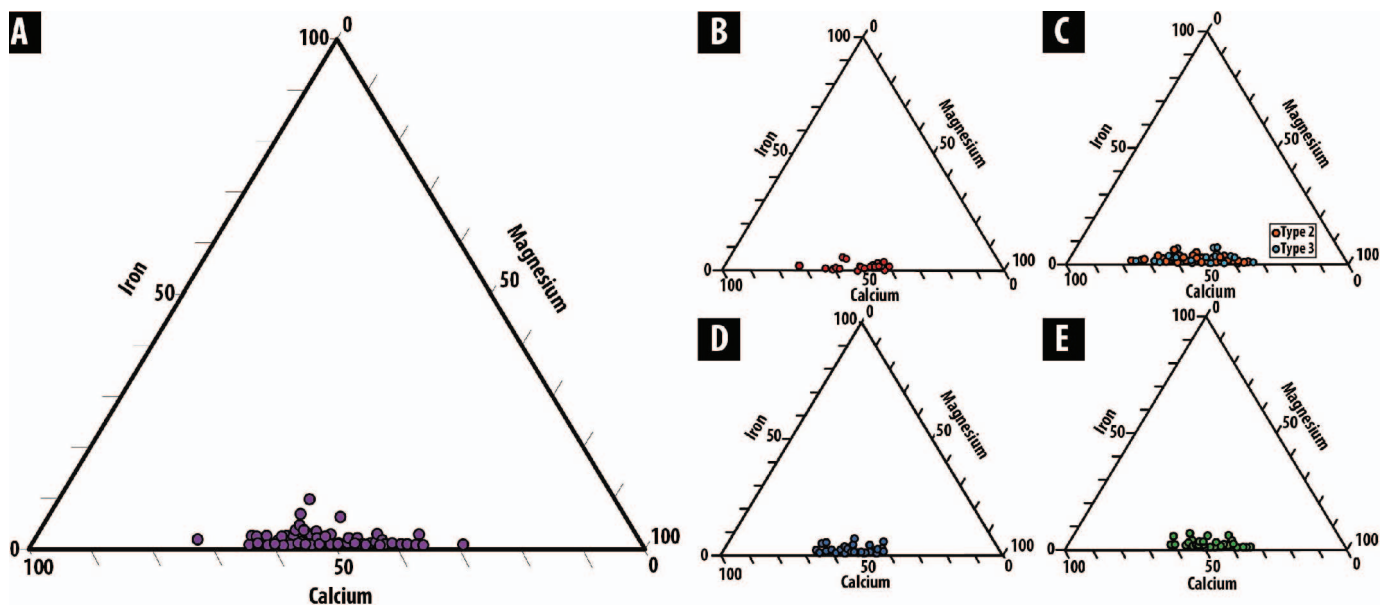


Fig. 8.—Ternary plot of the calcium, magnesium, and iron abundance in (mol %) middle Bakken dolomites. **A**) All data; **B**) Type 1 dolomites; **C**) Type 2 (red) and Type 3 (blue) dolomites; **D**) Type 4 dolomites; **E**) Type 6 dolomites. Type 7 dolomites were omitted due to their scarcity and fine nature.

The temperature histogram in Figure 11A suggests that the bulk of calcite cementation occurred between 15 and 20°C with steadily decreasing amounts at higher temperatures. Assuming a mean seawater temperature of 15°C, a geothermal gradient of 25°C/km, and an unchanging $\delta^{18}\text{O}_{\text{H}_2\text{O}}$, calcite cementation occurred at decreasing rates during burial to *ca.* 800

meters. Linking this to the burial history (Fig. 1), calcite cementation occurred over the first *ca.* 10 million years of burial. Given the occurrence of bioclasts in the middle Bakken and the carbon isotope signature of calcite ($0 \pm 3\text{‰}$), this calcite most likely represents the redistribution of biogenic calcite via local dissolution and precipitation.

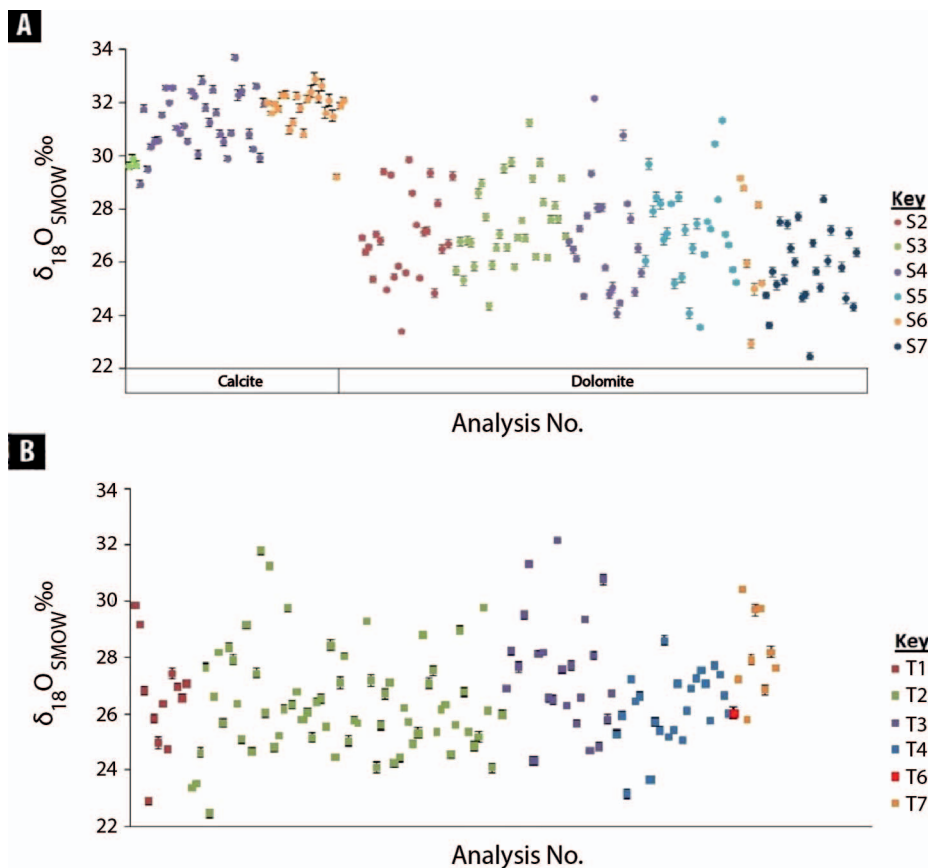


Fig. 9.—**A**) Grain-scale oxygen isotope data collected by SIMS, differentiated by sample (SIMS sample numbers S2–S7; see Table 1 for details of individual samples). Calcite and dolomite are separated for comparison. **B**) Grain-scale oxygen stable-isotope data collected by SIMS for dolomite differentiated by textural types T1–T6 (refer to Fig. 6 for textural types). Oxygen isotope data are reported relative to VSMOW. Error bars (2 SD) are plotted but are in most cases smaller than the data-point marker.

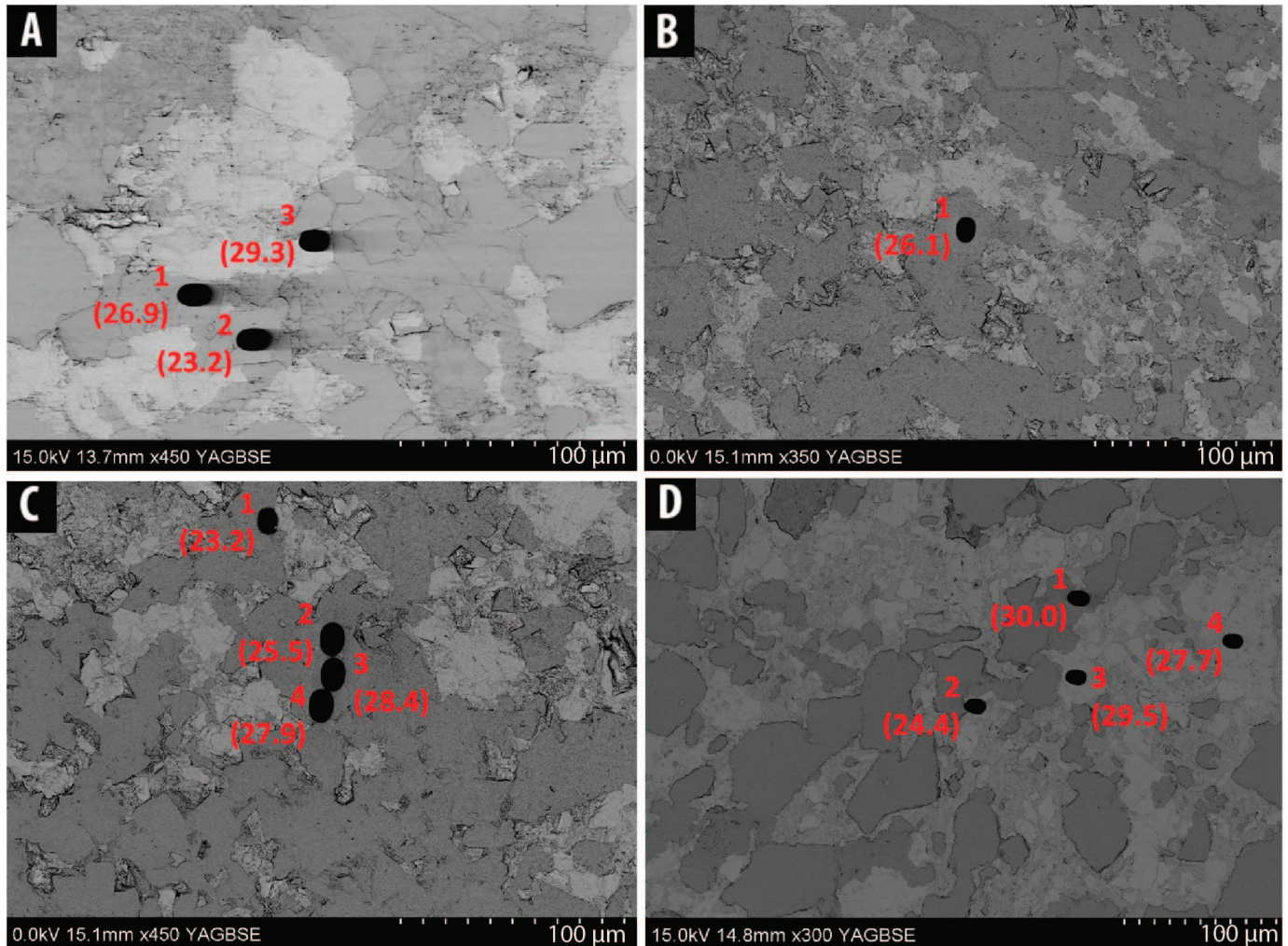


FIG. 10.—Secondary electron micrographs showing positions of SIMS analyses. $\delta^{18}\text{O}_{\text{SMOW}}$ values are labeled for each analysis. **A**) Analysis pits ablated from dolomite (1 and 2) and calcite (3), sample 2, sites 2-004 (1), 2-013 (2), and 2-081 (3) (excluded due to a boundary breach). **B**) An analysis pit at the center of the dolomite crystal, sample 1, site 1-051. **C**) four analysis pits; 2–4 were taken in a transect across a crystal of dolomite, sample 1, sites 1-073 (1), 1-071 (2), 1-071a (3), and 1-071b (4) (note that analysis 1 was excluded from the dataset due to a boundary break). **D**) Analysis pits from three crystals of dolomite (1) and calcite (2, 3, and 4), sample 3, sites 3-033 (1), 3-022 (2), 3-026 (3), 3-021 (4) (note that analyses 1 and 2 were excluded from the data set due to a boundary breaches). Refer to Table 1 and Supplemental Material for further information on each sample and individual sites.

Petrographic observations of (a) cloudy cores (transmitted light) and (b) porosity which likely results from the volume reduction associated with the replacement of calcite by dolomite (Weyl 1960), combined with (c) the inverse correlation between the amounts of dolomite and calcite, suggest that dolomite is largely replacing calcite rather than occurring as a pore-filling cement. In the absence of reaction fronts in individual crystals, it appears that dolomitization is a dissolution–precipitation reaction in which calcite is dissolved and 5–50-micrometer-size dolomite crystals are precipitated. The carbon isotope data for dolomite and calcite–dolomite mixtures are similar and are thus also consistent with dolomitization of calcite. Using the oxygen isotope paleothermometer proposed for dolomite by Vasconcelos et al. (2005) for dolomite–water and assuming, as a first estimate, that dolomite formed in unmodified seawater ($\delta^{18}\text{O}_{\text{H}_2\text{O}} = -1.5\text{‰}$), a temperature range of 13–66°C is calculated (Fig. 11B). Based on a correlation between $\delta^{18}\text{O}$ and the Ca content of diagenetic dolomites, Vahrenkamp et al. (1994) suggested that when estimating precipitation temperatures for dolomite, a correction of +0.1 per mil may be needed per mol % of Mg deficiency due to variations in mineral–water isotope fractionation factors. For most of our data, this results in a correction of

only < 0.3‰, with a maximum correction of 1.5‰; the range of estimated precipitation temperatures remains unchanged.

Since dolomite is supersaturated in seawater, dolomitization in unmodified seawater is geochemically feasible, but unusual (e.g., Machel 2004). Dolomitization more commonly occurs in fluids in which the Mg/Ca ratio has been modified as a result of evaporation and precipitation of gypsum (e.g., Budd 1997; Warren 2000; Machel 2004 for reviews). Anhydrite-bearing evaporites occur both below (Devonian Prairie Evaporite and Three Forks formations) and above (Mississippian Charles Salt Formation) the Bakken Formation, and pre-Mississippian waters in this part of the Williston basin are commonly hypersaline and are likely dolomitizing fluids (Iampen and Rostron 2000). Values of $\delta^{18}\text{O}$ for present-day formation waters from the Devonian Duperow aquifer, which occurs below the Bakken in this part of the Williston basin, are around +7.5 ‰ (Fig. 1A; Rostron and Holmden 2003). If we assume a value of +7.5‰, the maximum calculated precipitation temperature is 157°C, approximately that of the maximum burial temperature (Fig. 11D). If all dolomite formed from water with $\delta^{18}\text{O} = +7.5\text{‰}$, then precipitation temperatures range from 61 to 157°C (Fig. 11D). Slightly lower $\delta^{18}\text{O}$

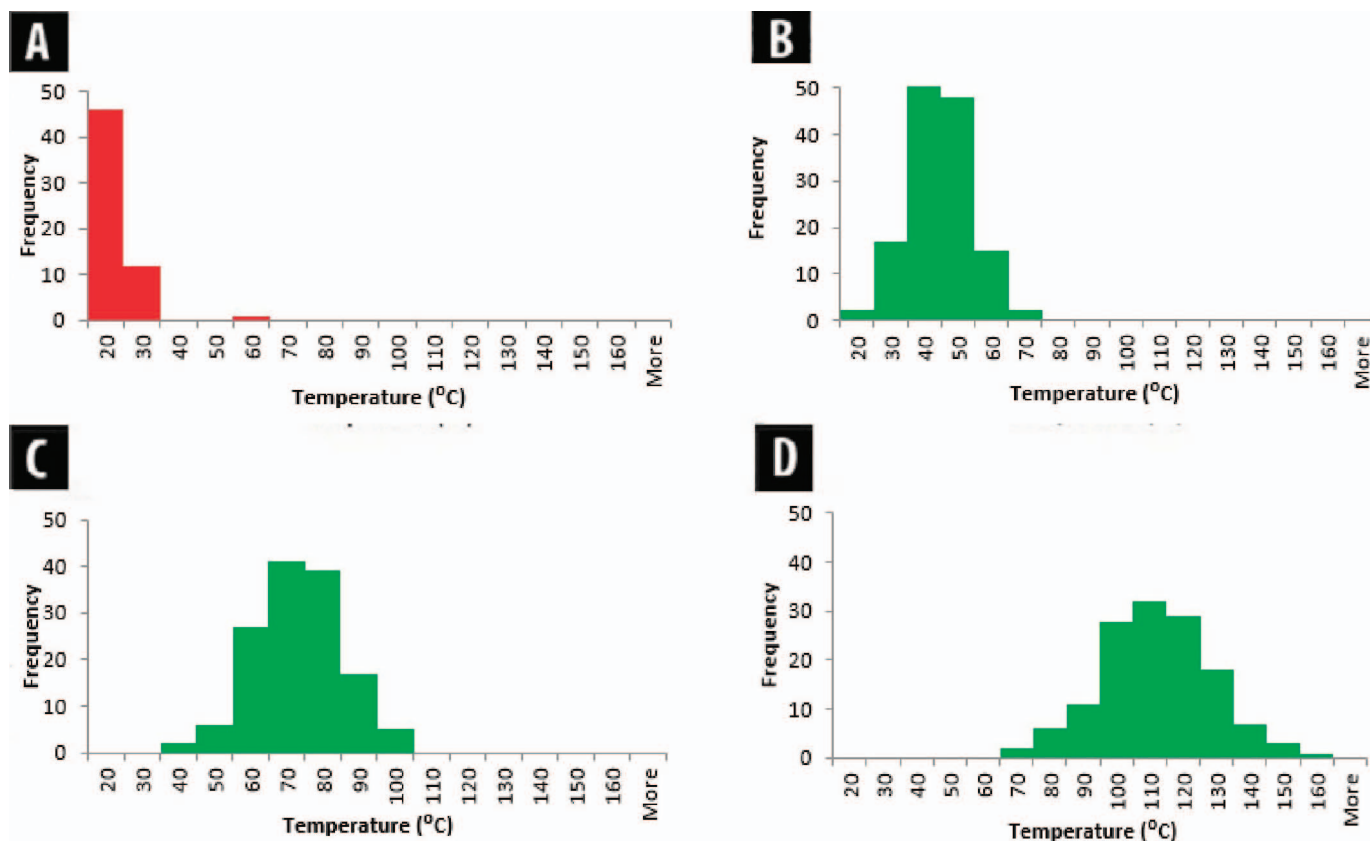


Fig. 11.—Histogram of calculated precipitation temperatures from SIMS $\delta^{18}\text{O}$ values for: **A)** calcite, assuming $\delta^{18}\text{O}_{\text{water}} = -1.5\%$; **B)** dolomite, assuming $\delta^{18}\text{O}_{\text{water}} = -1.5\%$; **C)** dolomite, assuming $\delta^{18}\text{O}_{\text{water}} = +3\%$; **D)** dolomite, assuming the $\delta^{18}\text{O}_{\text{water}} = +7.5\%$.

values, for example $+7\%$, would give a temperature range of $58\text{--}150^\circ\text{C}$. The histogram of estimated precipitation temperatures shows that the rate of dolomitization increases steadily from 60 to 130°C and then decreases at higher temperatures (Figure 11D). Given that dolomitization rates increase with temperature, the limited reaction at the highest temperatures might reflect the generation of petroleum from the organic-rich shales above and below the middle Bakken and its emplacement into the middle Bakken. If we assume that dolomitization occurred in fluids that evolved steadily from the original seawater (-1.5%) to the present-day brine ($+7.5\%$), then dolomite would have formed throughout almost the whole burial history of the Bakken (Figs. 1, 11). In either case, dolomitization occurred continuously over approximately $150\text{--}250$ million years.

The rate of dolomitization depends on a range of factors, including the Mg:Ca ratio in solution (Kaczmarek and Sibley 2007), the mineralogy of the reactant (Gaines 1974), and reactant surface area (Sibley et al. 1987). Rate constants for dolomite precipitation have been measured experimentally (Arvidson and Mackenzie 1999), and even at low diagenetic temperatures the resulting kinetics show that pervasive dolomitization and dolomite precipitation can occur on timescales of less than one million years (Whitaker and Xiao 2010; Al Helal et al. 2012); this is consistent with the occurrence of Holocene dolomites in modern sabkhas and carbonate islands (Budd 1997). Dolomitization rates increase markedly with increasing temperature (Arvidson and Mackenzie 1999) so that at the estimated temperatures of dolomitization in the Bakken ($61\text{--}157^\circ\text{C}$), rates are not controlled by kinetics. Rather, we suggest that the rate of dolomitization must be limited by the rate at which Mg is delivered to reaction sites and thus the fluid flow regime (Machel 2004; Whitaker et al. 2004). We have no way of evaluating the detailed flow history through the Bakken in North Dakota, but the highly saline and isotopically evolved

waters which occur in the region today are likely to be part of an ancient, highly restricted and almost stagnant flow system (Rostron and Holmden 2003). With no topographic recharge in the area, fluid flow would be driven almost entirely by sediment compaction, with very low water:rock ratios. The lack of fluid flow and related supply of Mg is the most likely reason why dolomitization, despite the length of time available for reaction, is partial rather than complete.

As in almost all diagenetic studies, the lack of constraint of paleo- $\delta^{18}\text{O}_{\text{H}_2\text{O}}$ limits our ability to generate highly constrained diagenetic time-temperature histories. In principle, clumped-isotope studies will allow this because precipitation temperatures can be fixed without the need to assume $\delta^{18}\text{O}_{\text{H}_2\text{O}}$ (Dale et al. 2014; Millán et al. 2016). However, the sample sizes currently required for clumped-isotope work precludes the grain-scale analyses such as those reported here. For the finely intergrown dolomites and calcites analyzed in this study, clumped isotopes would have yielded a range of temperatures depending on the mixture of calcite and dolomite grains drilled from each sample.

SUMMARY AND CONCLUSIONS

Shallow-marine fine-grained sandstones and siltstones from the Devonian middle Bakken Member are pervasively cemented with calcite and dolomite. Petrographic and mineralogical data show that dolomite occurs as a result of dolomitization of calcite.

The oxygen isotope composition of 57 individual calcite and 174 individual dolomite grains from six samples were determined using SIMS. A similarly wide range of values occurs in all six samples: 5% for calcite and 10% for dolomite. For dolomite, there is no relationship between

morphology, chemistry, and isotopic composition, so that in this case petrography is not a good guide to diagenetic history.

Since all samples display the same range of oxygen isotope values, we conclude that whilst carbonate diagenesis in the middle Bakken is heterogeneous on a millimeter scale, the same set of diagenetic processes are occurring on the same timescales on a 20-meter scale. Furthermore, the range of oxygen isotope compositions that occur on a millimeter scale are similar to the total ranges determined in many conventional isotope studies of carbonate-cemented sandstones sampled on scales greater than a meter. It is likely that either mixed phases or isotopically diverse single phases have been analyzed in previous studies, resulting in blurred or incorrect diagenetic histories.

A great benefit of SIMS is that through the generation of a large number of analyses of known phases, a much more accurate diagenetic history can be elucidated compared to conventional studies in which either sample numbers are restricted or there is uncertainty over what phases have been analyzed. In this study we can be confident that carbonate diagenesis has been almost continuous from deposition to maximum burial: a period of 300 million years. Within the uncertainty of $\delta^{18}\text{O}_{\text{H}_2\text{O}}$, calcite formed over the first *ca.* 10 Myr of burial, with most forming close to the sediment-water interface. Dolomitization occurred continuously from *ca.* 61–157°C over 150–250 million years. The rate of dolomitization was probably controlled by the rate of supply of Mg in a very sluggish flow regime; dolomitization is probably incomplete because of a lack of Mg and perhaps, in this case, by the fact that petroleum was emplaced into the sandstone late in the burial history.

SUPPLEMENTAL MATERIAL

Geochemistry of calcite and dolomite in the middle Bakken Formation, U.S.A. is available from JSR's Data Archive: <http://sepm.org/pages/asp?pageid=229>.

ACKNOWLEDGEMENTS

The authors are grateful to Statoil, who funded this work, and to the team at Wisconsin SIMS Laboratory for their assistance. WiscSIMS is supported by the National Science Foundation (EAR-1355590) and the University of Wisconsin–Madison. Our thanks are extended to the team at Scottish Universities Environmental Research Centre (SUERC) for assistance in obtaining bulk stable-isotope measurements. Thanks are also extended to KT Geoservices for XRD analysis. We thank reviewers Tony Buono and Sven Egenhoff, and AE Joe Macquaker, for their insightful comments, which focused and improved the manuscript. John Southard's editing is also very much appreciated.

REFERENCES

- AL-HELAL, A.B., WHITAKER, F.F., AND XIAO, Y., 2012, Reactive transport modeling of brine reflux: dolomitization, anhydrite precipitation, and porosity evolution: *Journal of Sedimentary Research*, v. 82, p. 196–215.
- APLIN, A.C., AND WARREN, E.A., 1994, Oxygen isotopic indications of the mechanisms of silica transport and quartz cementation in deeply buried sandstones: *Geology*, v. 22, p. 847–850.
- ARVIDSON, R.S., AND MACKENZIE, F.T., 1999, The dolomite problem: control of precipitation kinetics by temperature and saturation state: *American Journal of Science*, v. 299, p. 257–288.
- BJØRKUM, P.A., AND WALDERHAUG, O., 1990, Geometrical arrangement of calcite cementation within shallow marine sandstones: *Earth-Science Reviews*, v. 29, p. 145–161.
- BJØRKUM, P.A., AND WALDERHAUG, O., 1993, Isotopic composition of a calcite-cemented layer in the Lower Jurassic Bridport Sands, southern England: implications for formation of laterally extensive calcite-cemented layers: *Journal of Sedimentary Research*, v. 63, p. 678–682.
- BJØRLYKKE, K., 2014, Relationships between depositional environments, burial history and rock properties: some principal aspects of diagenetic process in sedimentary basins: *Sedimentary Geology*, v. 301, p. 1–14.
- BJØRLYKKE, K., AND JAHREN, J., 2012, Open or closed geochemical systems during diagenesis in sedimentary basins: constraints on mass transfer during diagenesis and the prediction of porosity in sandstone and carbonate reservoirs: *American Association of Petroleum Geologists, Bulletin*, v. 96, p. 2193–2214.
- BOGGS, S., AND KRINSLEY, D., 2006, *Application of Cathodoluminescence Imaging to the Study of Sedimentary Rocks*: Cambridge, UK, Cambridge University Press, 146 p.
- BRINT, J.F., HAMILTON, P.J., HASZELDINE, R.S., FALICK, A.E., AND BROWN, S., 1991, Oxygen isotopic analysis of diagenetic quartz overgrowths from the Brent sands: a comparison of two preparation methods: *Journal of Sedimentary Research*, v. 61, p. 527–533.
- BUDD, D.A., 1997, Cenozoic dolomites of carbonate islands: their attributes and origin: *Earth-Science Reviews*, v. 42, p. 1–47.
- BURLEY, S.D., MULLIS, J.T., AND MATTER, A., 1989, Timing diagenesis in the Tartan Reservoir (UK North Sea): constraints from combined cathodoluminescence microscopy and fluid inclusion studies: *Marine and Petroleum Geology*, v. 6, p. 98–120.
- CAVOSIE, A.J., VALLEY, J.W., AND WILDE, S.A., 2005, Magmatic $\delta^{18}\text{O}$ in 4400–3900 Ma detrital zircons: a record of the alteration and recycling of crust in the Early Archean: *Earth and Planetary Science Letters*, v. 235, p. 663–681.
- CURTIS, C.D., COLEMAN, M.L., AND LOVE, L.G., 1986, Pore water evolution during sediment burial from isotopic and mineral chemistry of calcite, dolomite and siderite concretions: *Geochimica et Cosmochimica Acta*, v. 50, p. 2321–2334.
- DALE, A., JOHN, C.M., MOZLEY, P.S., SMALLY, P.C., AND MUGGERIDGE, A.H., 2014, Time-capsule concretions: unlocking burial diagenetic processes in the Mancos Shale using carbonate clumped isotopes: *Earth and Planetary Science Letters*, v. 81, p. 278–293.
- EGENHOFF, S.O., 2017, The lost Devonian sequence: sequence stratigraphy of the middle Bakken member, and the importance of clastic dykes in the lower Bakken member shale, North Dakota, USA: *Marine and Petroleum Geology*, v. 81, p. 278–293.
- EGENHOFF, S.O., VAN DOLAH, A., JAFFRI, A., AND MALETZ, J., 2011, Facies architecture and sequence stratigraphy of the Middle Bakken Member, Williston Basin, North Dakota, in Robinson, L., LeFever, J., and Gaswirth, S., eds., *Bakken–Three Forks Petroleum System in the Williston Basin*: Rocky Mountain Association of Geologists, Guidebook, p. 27–47 (on CD).
- FERDOUS, H., 2001, Regional sedimentology and diagenesis of the Middle Bakken member: implications for reservoir rock distribution in southern Saskatchewan [Ph.D. Dissertation]: University of Saskatchewan, 467 p.
- FREISATZ, W.B., 1995, Fracture-enhanced porosity and permeability trends in the Bakken Formation, Williston Basin, western North Dakota: *Montana Geological Survey, 7th International Williston Basin Symposium*, p. 389–398.
- GAINES, A.M., 1974, Protodolomite synthesis at 100°C and atmospheric pressure: *Science*, v. 183, p. 518–520.
- GILES, M.R., ed., 1997, *Diagenesis: A Quantitative Perspective: Implications for Basin Modelling and Rock Property Prediction*: Dordrecht, Kluwer Academic Publishers, 526 p.
- GILES, M.R., INDRELIID, S.L., BEYNON, G.V., AND AMTHOR, J., 2000, The origin of large-scale quartz cementation: evidence from large data sets and coupled heat-fluid mass transport modelling, in Worden, R.H., and Morad, S., eds., *Quartz Cementation in Sandstones: International Association Sedimentologists, Special Publication 29*, p. 21–38.
- GIRARD, J.P., MUNZ, I.A., JOHANSEN, H., HILL, S., AND CANHAM, A., 2001, Conditions and timing of quartz cementation in Brent reservoirs, Hild Field, North Sea: constraints from fluid inclusions and SIMS oxygen isotope microanalysis: *Chemical Geology*, v. 176, p. 73–92.
- GOLDSTEIN, R.H., 2001, Fluid inclusions in sedimentary and diagenetic systems: *Lithos*, v. 55, p. 159–193.
- GLASMANN, J.R., LUNDERGARD, P.D., CLARK, R.A., PENNY, B.K., AND COLLINS, I.D., 1989, Geochemical evidence for the history of diagenesis and fluid migration: Brent Sandstone, Heather Field, North Sea: *Clay Minerals*, v. 24, p. 255–284.
- GLUYAS, J., AND COLEMAN, M., 1992, Material flux and porosity changes during sediment diagenesis: *Nature*, v. 356, p. 52–54.
- GRAHAM, C.M., VALLEY, J.W., AND WINTER, B.L., 1996, Ion microprobe analysis of $^{18}\text{O}/^{16}\text{O}$ in authigenic and detrital quartz in the St. Peter Sandstone, Michigan Basin and Wisconsin Arch, USA: contrasting diagenetic histories: *Geochimica et Cosmochimica Acta*, v. 60, p. 5101–5116.
- HART, B.S., LONGSTAFFE, F.J., AND PLINT, A.G., 1992, Evidence for relative sea-level change from isotopic and elemental composition of siderite in the Cardium Formation, Rocky Mountain Foothills: *Bulletin of Canadian Petroleum Geology*, v. 40, p. 52–59.
- HARWOOD, J., APLIN, A.C., FIALIPS, C.I., ILIFFE, J.E., KOZDON, R., USHIKUBO, T., AND VALLEY, J.W., 2013, Quartz cementation history of sandstones revealed by high-resolution SIMS oxygen isotope analysis: *Journal of Sedimentary Research*, v. 83, p. 522–530.
- HASZELDINE, R.S., SAMSON, I.M., AND CORNFORD, C., 1984, Dating diagenesis in a petroleum basin, a new fluid inclusion method: *Nature*, v. 307, p. 354–357.
- HOLLAND, F.D., JR., HAYES, M.D., THRASHER, L.C., AND HUBER, T.P., 1987, Summary of the biostratigraphy of the Bakken Formation (Devonian and Mississippian) in the Williston basin, North Dakota: Publisher is Saskatchewan Geological Society, 5th International Williston Basin Symposium, p. 68–76.
- HUDSON, J.D., AND ANDERSON, T.F., 1989, Ocean temperatures and isotopic compositions through time: *Royal Society of Edinburgh, Transactions, Earth Sciences*, v. 80, p. 183–192.
- IAMPEN, H.T., AND ROSTRON, B.J., 2000, Hydrogeochemistry of pre-Mississippian brines, Williston Basin, Canada–USA: *Journal of Geochemical Exploration*, v. 69, p. 29–35.
- KACZMAREK, S.E., AND SIBLEY, D.F., 2007, A comparison of nanometer-scale growth and dissolution features on natural and synthetic dolomite crystals: implications for the origin of dolomite: *Journal of Sedimentary Research*, v. 77, p. 424–432.

- KARASINKI, D.R., 2006, Sedimentology and hydrocarbon potential of the Devonian Three Forks and Mississippian Bakken Formations, Sinclair Area, southeast Saskatchewan–southwest Manitoba [Master's Thesis]: University of Manitoba, 436 p.
- KITA, N.T., USHIKUBO, T., FU, B., AND VALLEY, J.W., 2009, High precision SIMS oxygen isotope analyses and the effect of sample topography: *Chemical Geology*, v. 264, p. 43–57.
- KLEIN, J.S., MOZLEY, P., CAMPBELL, A., AND COLE, R., 1999, Spatial distribution of carbon and oxygen isotopes in laterally extensive carbonate-cemented layers: implications for mode of growth and subsurface identification: *Journal of Sedimentary Research*, v. 69, p. 184–201.
- KOZDON, R., USHIKUBO, T., KITA, N.T., SPICUZZA, M., AND VALLEY, J.W., 2009, Intratest oxygen isotope variability in the planktonic foraminifer *N. pachyderma*: real vs. apparent vital effects by ion microprobe: *Chemical Geology*, v. 258, p. 327–337.
- KUHN, P.P., DI PRIMO, R., HILL, R., LAWRENCE, J.R., AND HORSFIELD, B., 2012, Three-dimensional modeling study of the low-permeability petroleum system of the Bakken Formation: *American Association of Petroleum Geologists, Bulletin*, v. 96, p. 1867–1897.
- LAND, L.S., MILLIKEN, K.L., AND McBRIDE, E.F., 1987, Diagenetic evolution of Cenozoic sandstones, Gulf of Mexico sedimentary basin: *Sedimentary Geology*, v. 50, p. 195–225.
- LAST, W., AND EDWARDS, W., 1991, Petrology of the Middle Bakken Member in the Daly Field, southwestern Manitoba: Publisher is Saskatchewan Geological Society, 6th International Williston Basin Symposium, p. 64–69.
- LEE, M., AND SAVIN, S.M., 1985, Isolation of diagenetic overgrowths on quartz sand grains for oxygen isotopic analysis: *Geochimica et Cosmochimica Acta*, v. 49, p. 497–501.
- LI, H., HART, B., DAWSON, M., AND RADJEF, E., 2015, Characterizing the middle Bakken: laboratory measurement and rock typing of the middle Bakken Formation: *Unconventional Reservoirs Technology Conference*, 217485, 13 p., doi: 10.15530/URTEC-2015-2172485.
- LINZMEIER, B.J., KOZDON, R., PETERS, S.E., AND VALLEY, J.W., 2016, Oxygen isotope variability within growth bands suggests daily depth migration behavior is recorded in *Nautilus* shell aragonite: *PLOS One*, p. 1–31.
- LYON, I.C., BURLEY, S.D., MCKEEVER, P.J., SAXTON, J.M., AND MACAULAY, C., 2000, Oxygen isotope analysis of authigenic quartz in sandstones: a comparison of ion microprobe and conventional analytical techniques, in Worden, R.H., and Morad, S., eds., *Quartz Cementation in Sandstones*: International Association of Sedimentologists, Special Publication 29, p. 299–316.
- MACAULAY, C.I., HASZELDINE, R.S., AND FALICK, A.E., 1993, Distribution, chemistry, isotopic composition and origin of diagenetic carbonates: Magnus Sandstone, North Sea: *Journal of Sedimentary Petrology*, v. 63, p. 33–43.
- MACHEL, H.G., 2004, Concepts and models of dolomitization: a critical reappraisal, in Braithwaite, C.J.R., Rizzi, G., and Darke, G., eds., *The Geometry and Petrogenesis of Dolomite Hydrocarbon Reservoirs*: Geological Society of London, Special Publication 235, p. 7–63.
- MARCHAND, A.M., MACAULAY, C.I., HASZELDINE, R.S., AND FALICK, A.E., 2002, Pore water evolution in oilfield sandstones: constraints from oxygen isotope microanalyses of quartz cement: *Chemical Geology*, v. 191, p. 285–304.
- McBRIDE, E.F., AND MILLIKEN, K.L., 2006, Giant calcite-cemented concretions, Dakota Formation, central Kansas, USA: *Sedimentology*, v. 53, p. 1161–1179.
- MCCABE, H.R., 1959, Mississippian Stratigraphy of Manitoba: Manitoba, Department of Mines and Natural Resources, Mines Branch, Publication 58, 99 p.
- MEISSNER, F., 1978, Petroleum geology of the Bakken Formation Williston basin, North Dakota and Montana, in *The Economic Geology of the Williston Basin*: Montana Geological Society, 24th Annual Conference, Williston Basin Symposium, p. 207–227.
- MEISSNER, F.F., 1991, Petroleum Geology of the Bakken Formation Williston Basin, North Dakota and Montana: Montana Geological Society, Guidebook to Geology and Horizontal Drilling of the Bakken Formation, p. 19–42.
- MILLÁN, M.I., MACHEL, H., AND BERNASCONI, S.M., 2016, Constraining temperatures of formation and composition of dolimitizing fluids in the Upper Devonian Nisku Formation (Alberta, Canada) with clumped isotopes: *Journal of Sedimentary Research*, v. 86, p. 107–112.
- MURRAY, R.C., AND LUCIA, F.J., 1967, Cause and control of dolomite distribution by rock selectivity: *Geological Society of America, Bulletin*, v. 78, p. 21–36.
- O'NEIL, J.R., CLAYTON, R.N., AND MAYEDA, T.K., 1969, Oxygen isotope fractionation in divalent metal carbonates: *Journal of Chemical Physics*, v. 51, p. 5547–5558.
- OSBORNE, M., AND HASZELDINE, S., 1993, Evidence for resetting of fluid inclusion temperatures from quartz cements in oilfields: *Marine and Petroleum Geology*, v. 10, p. 271–278.
- PITMAN, J.K., PRICE, L.C., AND LEFEVER, J.A., 2001, Diagenesis and fracture development in the Bakken Formation, Williston Basin: implications for reservoir quality in the middle member: U.S. Geological Survey, Professional Paper 1653, 19 p.
- POLLINGTON, A.D., KOZDON, R., AND VALLEY, J.W., 2011, Evolution of quartz cementation during burial of the Cambrian Mount Simon Sandstone, Illinois Basin: *in situ* microanalysis of $\delta^{18}\text{O}$: *Geology*, v. 39, p. 1119–1122.
- ROBINSON, A., AND GLUYAS, J., 1992, Model calculations of loss of porosity in sandstones as a result of compaction and quartz cementation: *Marine and Petroleum Geology*, v. 9, p. 319–323.
- ROSTRON, B.J., AND HOLMDEN, C., 2003, Regional variations in oxygen isotopic compositions in the Yeoman and Duperow aquifers, Williston basin (Canada–USA): *Journal of Geochemical Exploration*, v. 78, p. 337–341.
- SCHMID, S., WORDEN, R.H., AND FISHER, Q.J., 2004, Diagenesis and reservoir quality of the Sherwood Sandstone (Triassic), Corrib field, Slyne basin, west of Ireland: *Marine and Petroleum Geology*, v. 21, p. 299–315.
- SIBLEY, D.F., 1982, The origin of common dolomite fabrics: clues from the Pliocene: *Journal of Sedimentary Petrology*, v. 52, p. 1087–1100.
- SIBLEY, D.F., AND GREGG, J.M., 1987, Classification of dolomite rock textures: *Journal of Sedimentary Petrology*, v. 57, p. 967–975.
- SIBLEY, D.F., DEDOES, R.E., AND BARTLETT, T.R., 1987, Kinetics of dolomitization: *Geology*, v. 15, p. 1112–1114.
- SIMENSON, A., 2010, Depositional Facies and Petrophysical Analysis of the Bakken Formation, Parshall Field, Mountrail County, North Dakota [Ph.D. Dissertation]: Colorado School of Mines, 190 p.
- ŚLIWIŃSKI, M.G., KITAJIMA, K., KOZDON, R., SPICUZZA, M.J., FOURNELLE, J.H., DENNY, A., AND VALLEY, J.W., 2016a, Secondary ion mass spectrometry bias on isotope ratios in dolomite–ankerite, Part I: $\delta^{18}\text{O}$ matrix effects: *Geostandards and Geoanalytical Research*, v. 40, p. 157–172.
- ŚLIWIŃSKI, M.G., KOZDON, R., KITAJIMA, K., DENNY, A., AND VALLEY, J.W., 2016b, Microanalysis of carbonate cement $\delta^{18}\text{O}$ in a CO_2 -storage system seal: insights into the diagenetic history of the Eau Claire Formation (Upper Cambrian), Illinois Basin: *American Association of Petroleum Geologists, Bulletin*, v. 100, p. 1003–1031.
- SMITH, M.G., AND BUSTIN, R.M., 1996, Production and preservation of organic matter during deposition of the Bakken Formation (Late Devonian and Early Mississippian), Williston Basin: *Palaeogeography, Palaeoclimatology, Palaeoecology*, v. 142, p. 185–200.
- STARJUALA, A., QING, H., CHI, G., STERN, R., AND PETTS, D., 2013, Dolomite petrography and stable isotope geochemistry of the Bakken Formation, southeastern Saskatchewan, in *Summary of Investigations, Volume 1, Saskatchewan Geological Survey, Saskatchewan Ministry of the Economy, Miscellaneous Report 2013-4.1, Paper A-8*, 10 p.
- SULLIVAN, M.D., MACAULAY, C.I., FALICK, A.E., AND HASZELDINE, R.S., 1997, Imported quartz cement in aeolian sandstone grew from water of uniform composition but has complex zonation: *Terra Nova*, v. 9, p. 237–241.
- TAYLOR, K.G., GAWTHORPE, R.L., CURTIS, C.D., MARSHALL, J.D., AND AWILLER, D.N., 2000, Carbonate cementation in a sequence-stratigraphic framework: Upper Cretaceous sandstones, Book Cliffs, Utah–Colorado: *Journal of Sedimentary Research*, v. 70, p. 360–372.
- TAYLOR, T.R., GILES, M.R., HATHON, L.A., DIGGS, T.N., BRAUNSDORF, N.R., BIRBIGLIA, G.V., KITTRIDGE, M.G., MACAULAY, C.I., AND ESPEJO, I.S., 2010, Sandstone diagenesis and reservoir quality prediction: models, myths, and reality: *American Association of Petroleum Geologists, Bulletin*, v. 94, p. 1093–1132.
- VAHRENKAMP, V.C., AND SWART, P.K., 1994, Late Cenozoic dolomites of the Bahamas: metastable analogues for the genesis of ancient platform dolomites, in Purser, B., Tucker, M., and Zenger, D., eds., *Dolomites: A Volume in Honour of Dolomieu*, International Association of Sedimentologists, Special Publication 21, p. 133–153.
- VALLEY, J.W., AND KITA, N.T., 2009, *In situ* oxygen isotope geochemistry by ion microprobe, in Fayek, M., ed., *Secondary Ion Mass Spectrometry in the Earth Sciences: Mineralogical Association of Canada, Short Course*, v. 41, p. 19–63.
- VAN GELDERN, R., JOACHIMSKI, M.M., DAY, J., JANSEN, U., ALVAREZ, F., YOLKIN, E.A., AND MA, X.P., 2006, Carbon, oxygen and strontium isotope records of Devonian brachiopod shell calcite: *Palaeogeography, Palaeoclimatology, Palaeoecology*, v. 240, p. 47–67.
- VASCONCELOS, C., MCKENZIE, J.A., WARTHMANN, R., AND BERNASCONI, S.M., 2005, Calibration of the $\delta^{18}\text{O}$ paleothermometer for dolomite precipitated in microbial cultures and natural environments: *Geology*, v. 33, p. 317–320.
- WARREN, J., 2000, Dolomite: occurrence, evolution and economically important associations: *Earth-Science Reviews*, v. 52, p. 1–81.
- WEBSTER, R.L., 1984, Petroleum source rocks and stratigraphy of the Bakken Formation in North Dakota, in Woodward, J., Meissner, F.F., and Clayton, J.L., eds., *Hydrocarbon Source Rocks of the Greater Rocky Mountain Region*: Rocky Mountain Association of Geologists, Symposium, p. 57–81.
- WEYL, P.K., 1960, Porosity through dolomitization: conservation of mass requirements: *Journal of Sedimentary Petrology*, v. 30, p. 85–90.
- WHITAKER, F.F., AND XIAO, Y., 2010, Reactive transport modeling of early burial dolomitization of carbonate platforms by geothermal convection: *American Association of Petroleum Geologists, Bulletin*, v. 94, p. 889–917.
- WHITAKER, F.F., SMART, P.L., AND JONES, G.D., 2004, Dolomitization: from conceptual to numerical models, in Braithwaite, C.J.R., Rizzi, G., and Darke, G., eds., *The geometry and petrogenesis of dolomite hydrocarbon reservoirs*: Geological Society of London, Special Publication 235, p. 99–139.
- WILKINSON, M., 1991, The concretions of the Bearerraig Sandstone Formation: geometry and geochemistry: *Sedimentology*, v. 38, p. 899–912.
- WILLIAMS, L.B., HERVIG, R.L., AND BJØRKYKKE, K., 1997, New evidence for the origin of quartz cements in hydrocarbon reservoirs revealed by oxygen isotope microanalyses: *Geochimica et Cosmochimica Acta*, v. 61, p. 2529–2538.